Carbohydrate Polymers 95 (2013) 57–63

Contents lists available at SciVerse ScienceDirect

Carbohydrate Polymers

journal homepage: www.elsevier.com/locate/carbpol

Effects of dissolution of some lignocellulosic materials with ionic liquids as green solvents on mechanical and physical properties of composite films

Ali Abdulkhani[a], Ebrahim Hojati Marvast[a], Alireza Ashori[b,*], Ali Naghi Karimi[a,c]

[a] Department of Wood and Paper Science and Technology, Faculty of Natural Resources, University of Tehran, Karaj, Iran
[b] Department of Chemical Technologies, Iranian Research Organization for Science and Technology (IROST), P.O. Box 15815-3538, Tehran, Iran
[c] Institute of Tropical Forestry and Forest Products (INTROP), University Putra Malaysia (UPM), 43400 Serdang, Selangor, Malaysia

ARTICLE INFO

Article history:
Received 7 November 2012
Received in revised form 1 February 2013
Accepted 21 February 2013
Available online 1 March 2013

Keywords:
Ionic liquids
Lignocellulosic biomass
[BMIM]Cl
[DiMIM][$MeSO_4$]
Dissolution
Physical and mechanical properties

ABSTRACT

In this study two imidazole-based ionic liquids (ILs), namely 1-butyl-3-methyl-1-imidazolium chloride ([BMIM]Cl) and 1,3-methyl imidazolium dimethyl sulfate ([DiMIM][$MeSO_4$]), were used to dissolve ball-milled poplar wood (PW), chemi-mechanical pulp (CMP), and cotton linter (CEL). A set of comparative experiments was carried out, and physical and mechanical properties of the composite films from three different raw materials were determined by means of optical transparency (OT), scanning electron microscopy (SEM), water absorption (WA), thickness swelling (TS), water vapor permeability (WVP), and tensile strength (σb). The overall evaluation indicates the inability of [DiMIM][$MeSO_4$] in complete dissolution of lignocellulosic materials, and sample treatment with this solvent did not lead to water soluble degradation products. However, dissolution trials using [BMIM]Cl were able to dissolve all used lignocellulosic materials by destroying inter and intramolecular hydrogen bonds between lignocelluloses. The OT, WA, TS, and σb of regenerated CEL films were much higher than those of CMP and PW composites. In addition, CEL film showed the lowest WVP compared to WF and CMP composite films. This work demonstrated a promising route for the preparation of biodegradable green cellulose composite films.

1. Introduction

The use of lignocellulosic biomass based materials in various sectors (e.g. automotive and aerospace) instead of petro-materials has received increased attentions due to the growing global environmental awareness, and concepts of sustainability and industrial ecology (Hamzeh, Ashori, Mirzaei, Abdulkhani, & Molaei, 2011; Moniruzzaman & Ono, 2012). Wood is a renewable source for cellulose, lignin, hemicelluloses and extractives (Mäki-Arvela, Anugwom, Virtanen, Sjöholm, & Mikkola, 2010). A lignocellulosic material contains 35–50% cellulose, up to 35% hemicelluloses, 5–30% lignin as well as a few percent of extractives (Lynd, Weimer, Van Zyl, & Pretorius, 2002). Cellulose is the most abundant biopolymer on the Earth and, thus, it is a valuable source of raw materials (Mäki-Arvela et al., 2010). It is formed via 1,4-β-D-glucose linkage of anhydroglucose units, and contains several inter- and intramolecular hydrogen bonds (Zhang, Wu, Zhang, & He, 2005), which should be broken during the dissolution of cellulose. Furthermore, native cellulose is considered as a rigid semi-crystalline material (Pinkert, Marsh, Pang, & Staiger, 2009). Lignin is a complex polymer composed of phenylpropanoid units consisting primarily of coniferyl, sinapyl and *p*-coumaryl alcohols. These components are assembled in a complex three-dimensional structure, remarkably resistant against chemicals and microbial attack that makes it very difficult to hydrolyze. The insolubility of wood in common solvents has severely hampered the development of new methods for the efficient utilization of wood and its components (Kilpeläinen et al., 2007). An effective dissociation of these components and their subsequent separation is needed for the production of high value products from lignocellulosic biomass (Hamzeh, Ashori, Khorasani, Abdulkani, & Abyaz, 2013). On the other side, if the biopolymers could be cleanly and easily separated from any lignocellulosic biomass source, they could serve as ready feedstock for not only polymeric composite materials, but also for base chemicals and fuels that are now obtained primarily from oil. The true biorefinery would not be based on production of only a fuel, but a rich, nearly limitless variety of chemicals (Fig. 1).

Traditionally, drastic conditions, such as strong base or mineral acids, are used to exploit the lignocellulosic materials. In these processes, the extracted fractions are severely and irreversibly altered, and environmental pollution is also of great concern. Moreover, conventional processes cannot make full use of non-cellulose

* Corresponding author. Tel.: +98 21 5627 6637; fax: +98 21 5627 6265.
E-mail address: ashori@irost.org (A. Ashori).

0144-8617/$ – see front matter © 2013 Elsevier Ltd. All rights reserved.
http://dx.doi.org/10.1016/j.carbpol.2013.02.040

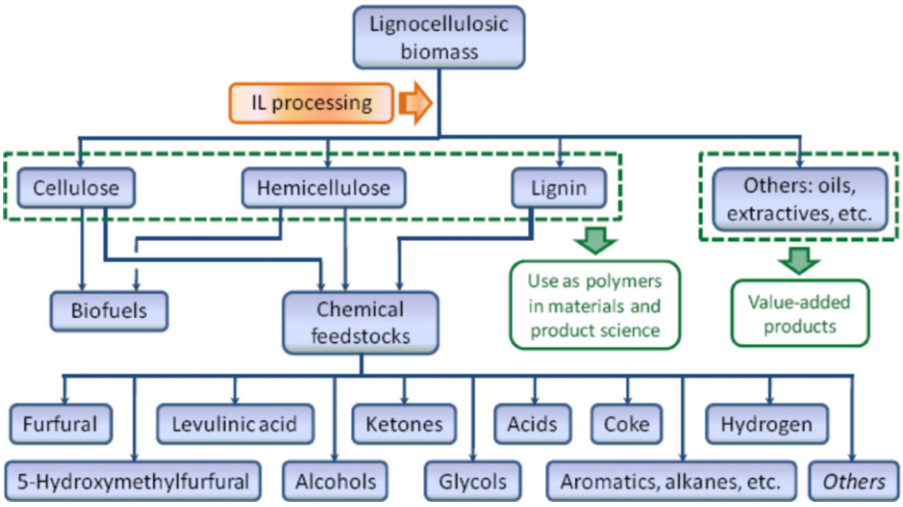

Fig. 1. Possible applications of the three major components from lignocellulosic biomass (Sun, 2010).

biopolymers, i.e. lignin and hemicelluloses. In order to overcome these obstacles, some mild processes and pretreatment are proposed, e.g. enzymatic hydrolysis, steam explosion, organic solvent, and ammonia fiber explosion (Öhgren, Bura, Saddler, & Zacchi, 2007; Yang, Zhong, Yuan, Peng, & Sun, 2013). However, this issue is still pending due to the high crystallinity of cellulose, relatively high reactivity of carbohydrates, insolubility of cellulose in conventional solvents and heterogeneity of lignocelluloses (Remsing, Swatloski, Rogers, & Moyna, 2006). Therefore, new technologies should be developed for the green bio-refinery of biomass resources.

In 2002, Swatloski et al. were the first to demonstrate that ionic liquids (ILs) are able to dissolve cellulose. However, in recent years the dissolution of lignocellulosic biomass in ILs has drawn a great deal of attention. ILs are organic salts entirely composed of cations (usually organic) and anions (usually inorganic) with generally low melting temperatures ($\leq$100 °C). They are green solvents, which are characterized by negligible vapor pressure as well as excellent thermal and chemical stability. The use of ILs as solvents has increased recently as a result of a globally growing interest toward green chemistry. Their unique properties make them attractive alternatives to conventional organic solvents in many chemical processes. Their use can provide a concrete solution to the problem of formation of volatile organic carbons (VOCs) in conventional solvents, which are detrimental to the environment (Anderson, Ding, Welton, & Armstrong, 2002). Many factors, e.g. species of biomass, particle size, water content, affect the dissolution of lignocellulosic materials in ILs (Li, Asikkala, Filpponen, & Argyropoulos, 2010; Sun, 2010). In addition, when the dissolving temperature is higher than the glass transition of lignin, the dissolution and fractionation of lignocelluloses can be more efficient (Li, Wang, & Zhao, 2008). The ILs have attracted increasing interest as media for dissolving cellulose from lignocellulosic biomass in the pretreatment step (Fukaya, Hayashi, Wada, & Ohno, 2008; Zavrel, Bross, Funke, Büchs, & Spiess, 2009). The dissolved cellulose in IL can be easily regenerated with the addition of an anti-solvent, such as water, ethanol or acetone (Zhu et al., 2006). As reported in the literature, apart from extracting cellulose from the primitive resources, regenerated cellulose exhibits significantly reduced crystallinity and increased porosity, which enhance the digestibility of the material and subsequently result in a higher yield for the overall conversion process (Li et al., 2011).

The aim of this work was to explore the influences of IL treatments on the fractionation process under mild conditions. The ILs [BMIM]Cl and [DiMIM][$MeSO_4$], which have been proved to be good solvents for lignocellulosic materials (Huddleston et al., 2001; Zhang, Deng, Li, & Chen, 2008), were used to directly dissolve the ball milling fibrous materials. Consequently, the resulting mixtures were used to make composite films, where they were characterized in terms of physical and mechanical properties.

2. Materials and methods

2.1. Raw materials and chemicals

The lignocellulosic materials (LMs) used for this study were poplar wood (*Popolus deltiodes*) (PW), chemi-mechanical pulp (CMP) of poplar, and cotton linter (CEL) containing 99% α-cellulose. The air-dried wood and pulp samples were ground in a 1 gal porcelain jar (rotary ball mill) using alumina balls under a nitrogen atmosphere. Consequently, they were oven-dried at 105 °C for 8 h and kept inside a sealed plastic bag. All the above-mentioned materials were procured from the local market.

Two imidazole-based ILs, namely 1-butyl-3-methyl-1-imidazolium chloride ([BMIM]Cl) and 1,3-metyl imidazolium dimethyl sulfate ([DiMIM][$MeSO_4$]), were synthesized according to the literature (Huddleston et al., 2001; Zhang et al., 2008). Fig. 2 shows the ^{13}C NMR spectra of laboratory synthesized ILs. All other chemical reagents were purchased from Merck, Germany.

2.2. ^{13}C NMR analysis

The NMR spectra of synthesized ILs were recorded on a JOEL JNM-ECX50 500 MHz spectrometer. IL solvents were placed in a 5-mm diameter NMR tube: a 75 pulse width, 1.4 s acquisition time, and 4 s relaxation delay were used. A total of 2000 scans were collected.

2.3. Dissolution process

Since water competes with the IL to establish hydrogen bonds, the presence of water in the solution water may decrease wood solubility in the ILs. Each lignocellulosic material and IL were placed in a flask under nitrogen filled environment and heated at 70–90 °C on a hot plate with magnetic stirring (200–500 rpm). The treatment conditions used for the respective prepared mixes are given in Table 1. The dissolution procedure of the materials was monitored using an optical microscopy with 10× magnification.

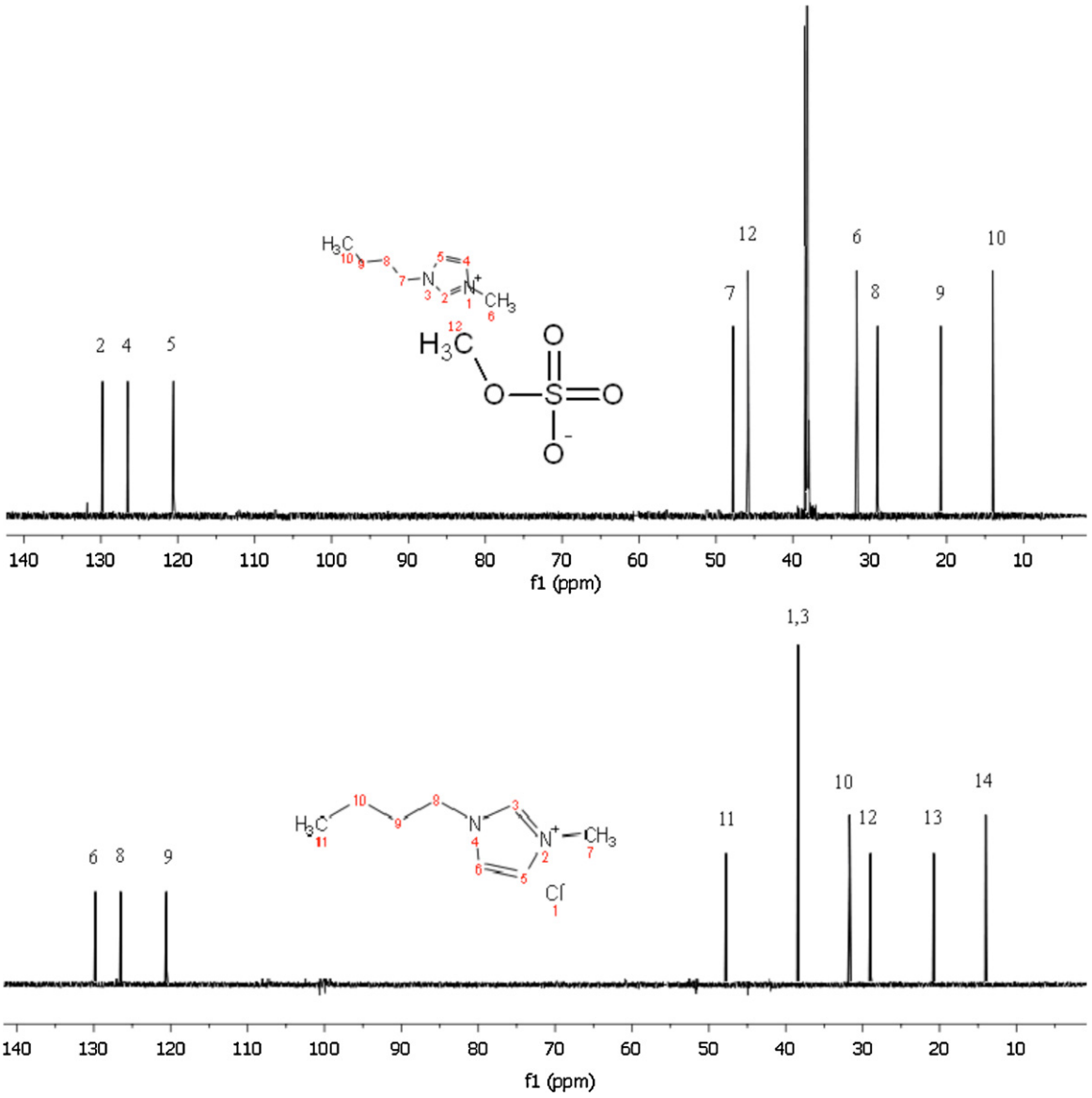

Fig. 2. ^{13}C NMR spectra of synthesized (a) [DiMIM][$MeSO_4$] and (b) [BMIM]Cl.

2.4. Preparation of composite films

The obtained almost transparent suspension was spread in a Petri dish with the diameter of 7.5 cm to give a ca. 2 mm thick layer. Subsequently, the air bubbles were removed in a vacuum oven (at 100 °C and for 30 min). The composite gel was slowly formed, and further kept in the ambient temperature for 2 days. Then, the composite gel was washed with running deionized water to remove the IL, and air-dried at ambient temperature. A series of films with different weight ratios were obtained by this method (Fig. 3).

Table 1
Treatment conditions for various fibrous materials.

Materials	LM/IL[a]	Mixing (rpm)	Time (h)	Temp. (°C)
PW	1/10	500–250	4	70–90
CMP	1/20	500–200	2	70–90
CEL	1/25	500–100	0.5	70–90

[a] w/w.

2.5. Testing

2.5.1. Physical properties

2.5.1.1. Optical transparency (OT). The percentage of OT or optical transmittance of the composite films was measured with a visible lux meter (Testo 540, UK). The thickness of the composites was about 0.5 mm. The results are the average of at least 5 specimens from each composite.

2.5.1.2. Water absorption (WA) and thickness swelling (TS). The WA and TS tests were conducted in accordance with ASTM D570. Before testing, the weight and dimensions of each specimen were measured. Conditioned samples of each type of composite were fully immersed in distilled water at 60 °C for 1, 6, 24, 48 and 72 h. Samples were removed from the water at certain time, patted dry and then measured again. The sample dimensions were 1.5 cm × 1 cm × 0.5 mm. A minimum of three samples was tested for each composite.

2.5.1.3. Water vapor permeability (WVP). WVP tests were carried out according to ASTM E96. The films were cut into circles, sealed

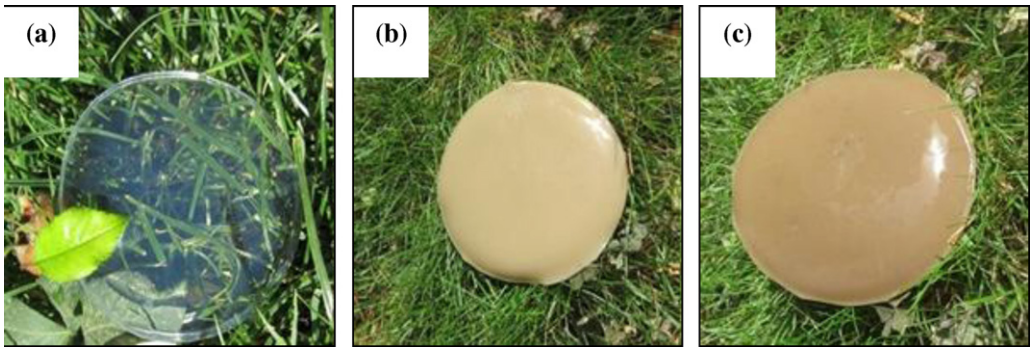

Fig. 3. Composite films of (a) CEL, (b) CMP, and (c) PW.

over with melted paraffin, and conditioned in a desiccator at 20 °C. RH 0 was maintained using anhydrous calcium chloride ($CaCl_2$) in the cell. Each cell was placed in a desiccator, containing saturated sodium chloride, to provide a constant RH of 65%. Water vapor transport was determined by the weight gain of the permeation cell. Changes in the weight of the cell were recorded as a function of time. Slopes were calculated by linear regression (weight change vs. time) and correlation coefficients for all reported data were >0.99. The water vapor transpiration rate (WVTR) is defined as the slope (g/s) divided by the transfer area (m^2). After the permeation tests, film thickness was measured and WVP (g/smPa) was calculated according to the following equation:

$$\mathrm{WVP} = \frac{\mathrm{WVTR}}{P(R_1 - R_2)}.x \quad (1)$$

where P is the saturation vapor pressure of water (Pa) at the test temperature (20 °C), R_1 is the RH in the desiccator, R_2 is the RH in the permeation cell and x is the film thickness (m). Under these conditions, the driving force $[P(R_1 - R_2)]$ was 1753.55 Pa.

2.5.1.4. Morphological study. Studies on the morphology of the composite films were carried out using a scanning electron microscopy (SEM). SEM micrographs of the surfaces of specimens were taken using SEM model Philips XL 30 at 17 kV accelerating voltage. The oven-dried specimens were mounted on SEM holder using double sided electrically conducting carbon adhesive tabs to prevent surface charge on the specimens when exposed to the electron beam.

2.5.2. Mechanical properties

After conditioning (20 ± 1 °C, 65 ± 5% RH) for at least 2 weeks, all the specimens were tested following ASTM D882-83. The tensile strength (σb) and elongation at break (εb) of the films were measured on a universal testing machine (Testometric M350-10CT) at a crosshead speed of 10 mm/min. The distance between the jaws was set at 1 mm. Composite films were cut in strips about 0.5 mm thick, 5 mm wide and 20 mm long. The σb and εb values are the averages of 5 measurements.

3. Results and discussion

3.1. Physical properties

3.1.1. Dissolution

The dissolution of PW, CMP and CEL materials in ILs was studied. The treatment with [DiMIM][$MeSO_4$] had no obvious effect on the solubility of the PW films. The wood chips swelled shortly after they were added to the [BMIM]Cl solvent. After heating for 2–3 h at 90 °C

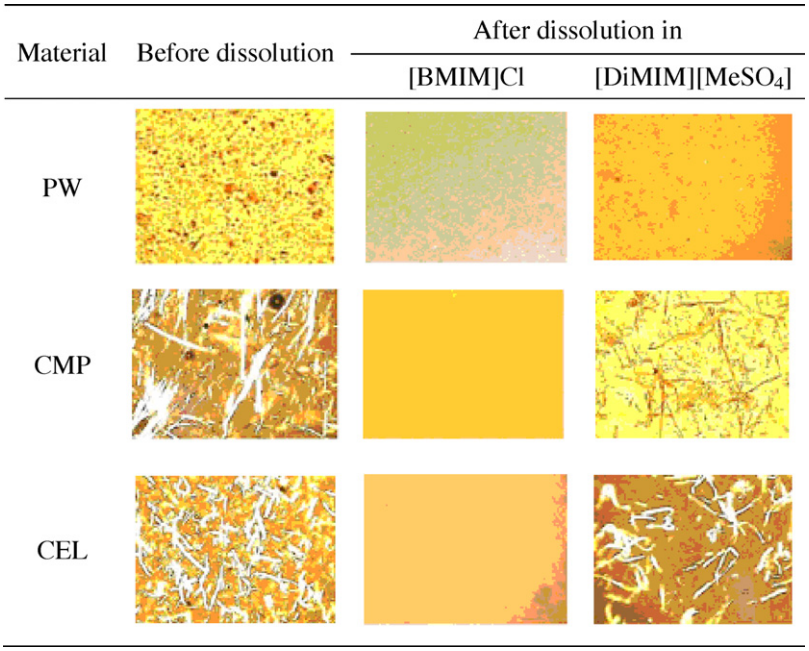

Fig. 4. Images of untreated and treated lignocellulosic materials in used ILs.

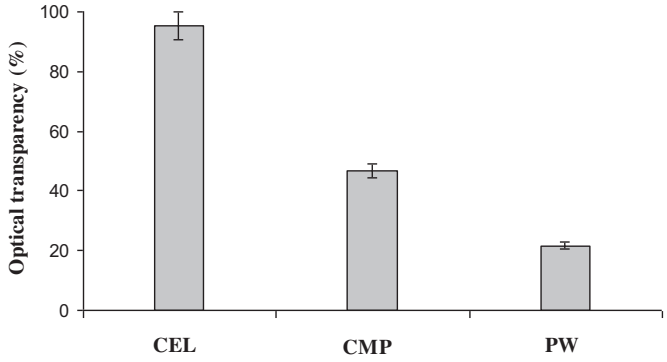

Fig. 5. Optical transparency of composite films.

under vigorous mechanical stirring, color of the solutions turned dark and their viscosities distinctively increased, indicating that the dissolution of wood had occurred. A clear, dark brown solution was obtained after filtration, and the brown gel was reconstituted by the addition of water; after washing several times with water, the gel became white, indicating that its main components were carbohydrates. An optical microscope was used to observe the dissolution process of wood chips in ILs (Fig. 4). In case of [DiMIM][$MeSO_4$] treatment, result shows that the PW and CMP samples were in their original states and fibrous structures. The dissolution rate increased at 90 °C; and at this temperature, most of the fibrous material disappeared after only 30 min and the visual field became light. Even at 110 °C, no further changes were observed; a fully black field was not obtained even when the reaction time was increased to 4 h. In general, the experiments consistently indicate that [DiMIM][$MeSO_4$] can only partially dissolve wood chips. ILs are capable of dissolving complex macromolecules and polymeric materials with high efficiency by breaking the extensive hydrogen bonding network of polysaccharides and promoting their dissolution (Swatloski, Spear, Holbrey, & Rogers, 2002).

The dissolving process of CEL in [BMIM]Cl at 80 °C was monitored using an optical microscopy. It was very interesting to observe that the CEL, without being pretreated or activated, could be dissolved in [BMIM]Cl within 45 min. The solubilization efficiency of lignocellulosic materials in ILs was found to be in the order of CEL > CMP ≥ PW. It is probably due to the high crystallinity of cellulose and the aromatic character of lignin (Kilpeläinen et al., 2007). It was also observed that the viscosity of the solution mainly depends on the content of cellulose, and the higher the content of cellulose, the higher the viscosity of the solution.

3.1.2. Optical transparency

Usually, transparency is a useful criterion for the miscibility and compatibility of the composite elements (Li et al., 2011). The optical transmittance of the films is shown in Fig. 5. The composite films prepared with the CEL exhibited excellent optical transmittance, indicating perfect miscibility. As expected, the CMP and PW films had relatively low transparency values (40% and 20%, respectively). When the content of lignin content was high enough, the aggregate could be formed. Thus, the particle aggregates led to the scattering caused by large particles, resulting in the decrease of transparency. These results could also explain the phenomenon shown in the dissolution process.

3.1.3. Water sorption and thickness swelling

Water uptake is one of the major issues that limits the applications of cellulose based materials, as this impacts dimensional stability, mechanical property stability, and chemical stability, and has been recently reviewed (Dufresne, 2008; Moon, Martini, Nairn, Simonsen, & Youngblood, 2011). Fig. 6 shows the percentages of the WA for the composites at different periods of immersion. Based on the test results, WA values ranged from 114% to 120% for PW film and from 32% to 42% for CEL film. Weight gain upon exposure to water increased as the immersion time increased for all the tested composites. It is to be noted that the maximum WA occurred during the first immersion time. This was possible due to the hydrogen bonding of the water molecules to the free hydroxyl groups present in the cellulosic cell wall of fibrous materials and the diffusion of water molecules into the microfibrils interfaces. Additionally, large number of porous tubular structures present in poplar fibers can accelerate the penetration of water by the so-called capillary action. From chemical view, this result could be explained by the highly differing chemical compositions of PW compared to CEL and CMP. CEL contains lower free hydroxyl groups, therefore it would be expected to show lower water uptake compared to PW.

The TS is an important property that represents the stability performance of the composite. The TS of the films increases with the WA and thus has a similar trend to the WA. As mentioned earlier, the poor absorption resistance of the cellulosic materials is mainly due to the presence of polar groups, which attract water molecules through hydrogen bonding. This phenomenon leads to a moisture build-up in the fiber cell wall (fiber swelling) and also in the microfibrils interfaces. This is responsible for the changes in the dimension of composites, particularly the thickness and the linear expansion due to reversible and irreversible swelling of the composites. As it can be seen in Fig. 6, the TS increased sharply during the first hour of immersion. A further increase in immersion time

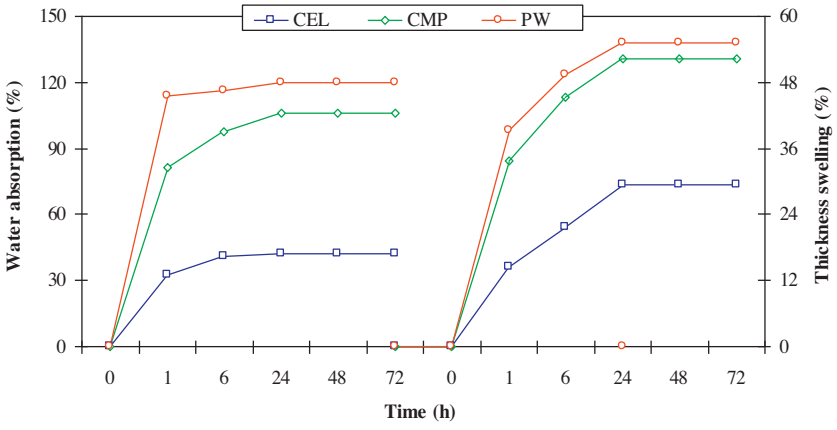

Fig. 6. Water absorption and thickness swelling of composite films.

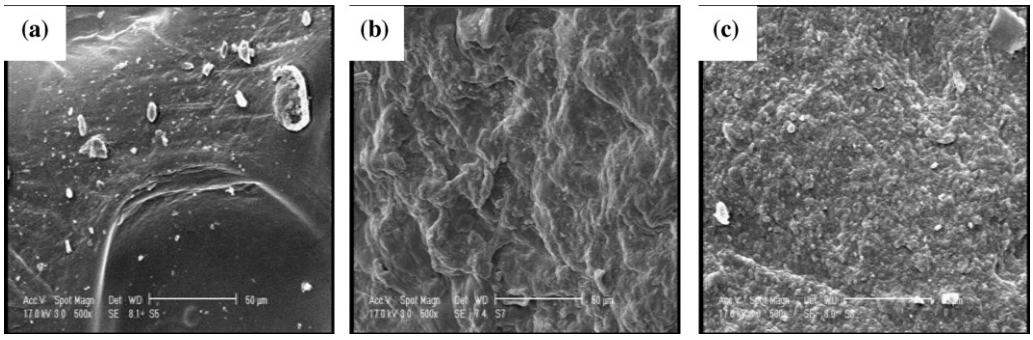

Fig. 7. SEM micrographs of the surfaces of (a) CEL, (b) CMP, and (c) PW films.

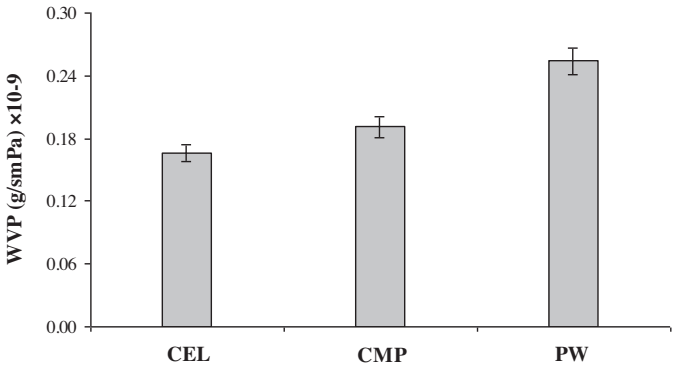

Fig. 8. Tensile strength of composite films.

showed a little change (increase) in the dimensional stability of films. Like WA, the CEL composites exhibited inferior dimensional stability compared to the PW composite. For example, the maximum value of TS was 55% for PW film, while the value for CEL film was 29%. As mentioned earlier, this is probably due to several reasons in terms of chemical compositions.

3.1.4. SEM characterization

SEM images of the surfaces for composite films are shown in Fig. 7. From these micrographs, it is clear that the CEL film has a smooth surface (Fig. 7(a)). It suggested that the cellulose nano-particles were embedded in the regenerated cellulose matrix because of the strong interaction between cellulose fibrils. However, as the content of lignin and hemicelluloses increased, the composite films gave increasingly rough surface, indicating that certain phase separation occurred here (Fig. 7(b) and (c)). In addition, the particles shown on the surface of composite fibrils have a very broad size (diameter) distribution, ranging from a few hundred nano-meters to the micron level. Cellulosic fibers used in this study can be roughly categorized as mixtures of nano-fibrils and micro-fibrils based on their diameters. The fibril lengths also show a broad distribution.

3.1.5. WVP

As a food packaging, film is often required to avoid or at least decrease moisture transfer between the food and the surrounding atmosphere, with water vapor permeability as low as possible. As shown in Fig. 8, WVP in CEL, CMP and PW films increased with the increase in contents of impurities (such as lignin and hemicelluloses). Water vapor easily went through PW film with the highest WVP values of 0.25×10^{-9} (g/smPa), while WVP value of CEL films reached 0.17×10^{-9} (g/smPa). The effect of decrement of the interstice is a decrease in WVP with the increasing of cellulose contents. With the increase of lignin content, WVP values increased gradually. The presence of lignin and hemicelluloses probably introduced a tortuous path for water molecules to pass through (Kristo & Biliaderis, 2007). At a low content of lignin (as filler), cellulosic fibers dispersed well as matrix (as shown by SEM), and blocked the water vapor. However, superfluous filler was easy to congregate (as shown in Fig. 7), which actually decreased the effective contents of filler and facilitated the WVP.

3.2. Mechanical properties

The mechanical properties of the composite materials, which can provide important information about the internal structure

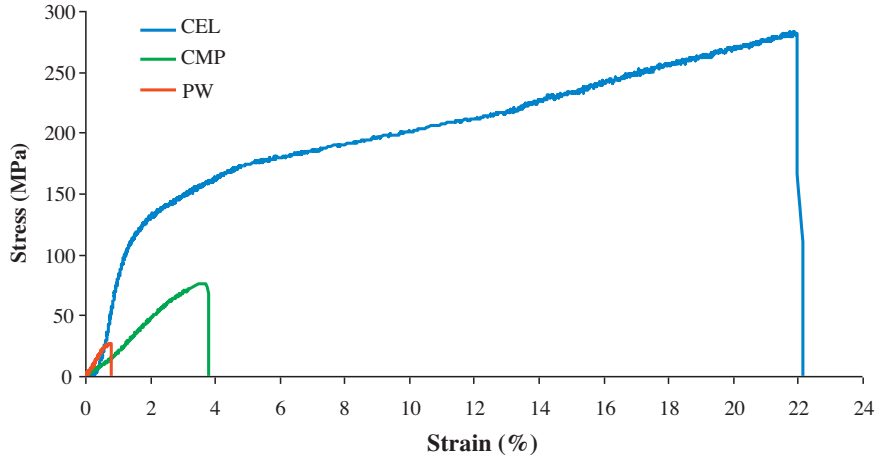

Fig. 9. The effect of lignocellulosic materials on water vapor permeability of the composite films.

Table 2
Mechanical properties of composite films.

Material	Tensile strength (MPa)	Young's modulus (MPa)	Elongation at break (%)
CEL	129.7	115.6	24.7
CMP	61.3	25.7	3.9
PW	17.8	41.7	1.2

of materials, are strongly influenced by the microstructure. Stress–strain curves of all the composite films are shown in Fig. 9. Table 2 shows the average values of tensile properties of CEL, CMP and PW films. As it can be seen, the CEL film underwent the most significant changes with a large increase in tensile strength, Young's modulus and elongation at break, indicating the cellulose matrix taken on the sufficient stress transfer as a result of stiffness of the self-reinforced material. Obviously, the presence of the lignin and hemicelluloses (as impurities) in the cellulose matrix has led to the weakening of the materials. It can be seen that with the increase of cellulose concentration, tensile strength of films increases. However, when lignin content is increased to a high level (i.e. PW sample), the strength of films does not increase with the increase in cellulose content, indicating that lignin has negative effect on tensile strength and elongation at high cellulose content. Based on these results, the interactions among cellulose and lignin demonstrate that optimal strength can be achieved with higher cellulose content and lower level of lignin content. In summary, each biopolymer not only contributes to the properties of composite films, but also engages in biopolymer–biopolymer interactions, which affect the mechanical properties of overall systems.

4. Conclusions

The present study not only realized an environmentally friendly method of cleanly extracting cellulose from woody materials under mild conditions, but also provided a new approach for utilizing biomass resources. Some conclusions of IL treatment are as follows:

(a) Different types of woody materials result in various dissolution profiles in ILs. In this work, CEL was found to be more suitable for dissolution and regeneration in both of the ILs used than the other two types of lignocellulosic materials.
(b) The results suggest that the optimal flexibility can be achieved at higher cellulose content with low level of lignin content.
(c) The solubilization efficiency of lignocellulosic materials in ILs was found to be in the order of CEL > CMP ≥ PW. It is probably due to the high crystallinity of cellulose and the aromatic character of lignin.
(d) Cellulose can greatly enhance the flexibility of films especially at low lignin contents.
(e) In general, mechanical and physical properties of CEL films were significantly higher than those of CMP and PW samples.
(f) The different WA and TS among all manufactured films can be attributed to the role of chemical components (such as cellulose, hemicelluloses, and lignin).
(g) Results show that [BMIM]Cl dissolves CMP and PW by destroying inter and intramolecular hydrogen bonds between lignocelluloses.

References

Anderson, J. L., Ding, J., Welton, T., & Armstrong, D. W. (2002). Characterizing ionic liquids on the basis of multiple solvation interactions. *Journal of the American Chemical Society*, *124*(47), 14253–14254.

Dufresne, A. (2008). Polysaccharide nanocrystal reinforced nanocomposites. *Canadian Journal of Chemistry*, *86*(6), 484–494.

Fukaya, Y., Hayashi, K., Wada, M., & Ohno, H. (2008). Cellulose dissolution with polar ionic liquids under mild conditions: Required factors for anions. *Green Chemistry*, *10*(1), 44–46.

Hamzeh, Y., Ashori, A., Khorasani, Z., Abdulkani, A., & Abyaz, A. (2013). Pre-extraction of hemicelluloses from bagasse fibers: Effects of dry-strength additives on paper. *Industrial Crops and Products*, *43*(5), 365–371.

Hamzeh, Y., Ashori, A., Mirzaei, B., Abdulkhani, A., & Molaei, M. (2011). Current and potential capabilities of biomass for green energy in Iran. *Renewable & Sustainable Energy Review*, *15*(9), 4934–4938.

Huddleston, J. G., Visser, A. E., Reichert, W. M., Willauer, H. D., Broker, G. A., & Rogers, R. D. (2001). Characterization and comparison of hydrophilic and hydrophobic room temperature ionic liquids incorporating the imidazolium cation. *Green Chemistry*, *3*(4), 156–164.

Kilpeläinen, I., Xie, H., King, A., Granstrom, M., Heikkinen, S., & Argyropoulos, D. S. (2007). Dissolution of wood in ionic liquids. *Journal of Agricultural and Food Chemistry*, *55*(22), 9142–9148.

Kristo, E., & Biliaderis, C. G. (2007). Physical properties of starch nanocrystal-reinforced pullulan films. *Carbohydrate Polymers*, *68*(1), 146–158.

Li, B., Asikkala, J., Filpponen, I., & Argyropoulos, D. S. (2010). Factors affecting wood dissolution and regeneration of ionic liquids. *Industrial and Engineering Chemistry Research*, *49*(5), 2477–2484.

Li, C., Wang, Q., & Zhao, Z. K. (2008). Acid in ionic liquid: An efficient system for hydrolysis of lignocelluloses. *Green Chemistry*, *10*(2), 177–182.

Li, W. Y., Sun, N., Stoner, B., Jiang, X. Y., Lu, X. M., & Rogers, R. D. (2011). Rapid dissolution of lignocellulosic biomass in ionic liquids using temperatures above the glass transition of lignin. *Green Chemistry*, *13*(8), 2038–2047.

Lynd, L. R., Weimer, P. J., Van Zyl, W. H., & Pretorius, I. S. (2002). Microbial cellulose utilization: Fundamentals and biotechnology. *Microbiology and Molecular Biology Reviews*, *66*(3), 506–577.

Mäki-Arvela, P., Anugwom, I., Virtanen, P., Sjöholm, R., & Mikkola, J. P. (2010). Dissolution of lignocellulosic materials and its constituents using ionic liquids—A review. *Industrial Crops and Products*, *32*(3), 175–201.

Moniruzzaman, M., & Ono, T. (2012). Ionic liquid assisted enzymatic delignification of wood biomass: A new 'green' and efficient approach for isolating of cellulose fibers. *Biochemical Engineering Journal*, *60*, 156–160.

Moon, R. J., Martini, A., Nairn, J., Simonsen, J., & Youngblood, J. (2011). Cellulose nanomaterials review: Structure, properties and nanocomposites. *Chemical Society Reviews*, *40*(7), 3941–3994.

Öhgren, K., Bura, R., Saddler, J., & Zacchi, G. (2007). Effect of hemicellulose and lignin removal on enzymatic hydrolysis of steam pretreated corn stover. *Bioresource Technology*, *98*(13), 2503–2510.

Pinkert, A., Marsh, K. N., Pang, S., & Staiger, M. P. (2009). Ionic liquids and their interactions with cellulose. *Chemical Reviews*, *109*(12), 6712–6728.

Remsing, R. C., Swatloski, R. P., Rogers, R. D., & Moyna, G. (2006). Mechanism of cellulose dissolution in the ionic liquid 1-n-butyl-3-methylimidazolium chloride: A ^{13}C and $^{35/37}Cl$ NMR relaxation study on model systems. *Chemical Communication*, *12*, 1271–1273.

Sun, N. (2010). *Dissolution and processing of cellulose materials with ionic liquids: Fundamentals and applications*. Ph.D. dissertation. Department of Chemistry, The University of Alabama, USA.

Swatloski, R. P., Spear, S. K., Holbrey, J. D., & Rogers, R. D. (2002). Dissolution of cellulose with ionic liquids. *Journal of the American Chemical Society*, *124*(18), 4974–4975.

Yang, D., Zhong, L.-X., Yuan, T.-Q., Peng, X.-W., & Sun, R.-C. (2013). Studies on the structural characterization of lignin, hemicelluloses and cellulose fractionated by ionic liquid followed by alkaline extraction from bamboo. *Industrial Crops and Products*, *43*(1), 141–149.

Zavrel, M., Bross, D., Funke, M., Büchs, J., & Spiess, A. C. (2009). High-throughput screening for ionic liquids dissolving (ligno-)cellulose. *Bioresource Technology*, *100*(9), 2580–2587.

Zhang, D. L., Deng, Y. F., Li, C. B., & Chen, J. (2008). Separation of ethyl acetateethanol azeotropic mixture using hydrophilic ionic liquids. *Industrial and Engineering Chemistry Research*, *47*(6), 1995–2001.

Zhang, H., Wu, J., Zhang, J., & He, J. (2005). 1-Allyl-3-methylimidazolium chloride room temperature ionic liquid: A new and powerful nonderivatizing solvent for cellulose. *Macromolecules*, *38*(20), 8272–8277.

Zhu, S., Wu, Y., Chen, Q., Yu, Z., Wang, C., Jin, S., et al. (2006). Dissolution of cellulose with ionic liquids and its application: A mini review. *Green Chemistry*, *8*(4), 325–327.